12-20-1994

X-Ray Absorption Studies of Strain in Epitaxial (Si-Ge) Atomic Layer Superlattice and Alloy Films

T. Tyliszczak
McMaster University, tolek@mcmaster.ca

A. P. Hitchcock
McMaster University

Z. H. Lu
National Research Council, Ottawa

J. -M. Baribeau
National Research Council, Ottawa

T. E. Jackman
McMaster University

Utah State University
MERRILL-CAZIER LIBRARY

X-RAY ABSORPTION STUDIES OF STRAIN IN EPITAXIAL (Si-Ge) ATOMIC LAYER SUPERLATTICE AND ALLOY FILMS

T. Tyliszczak[1,*], A.P. Hitchcock[1], Z.H. Lu[2], J.-M. Baribeau[2] and T.E. Jackman[1,2]

[1]Institute for Materials Research, McMaster University, Hamilton, Ont. Canada L8S 4M1
[2]Institute for Microstructural Sciences, National Research Council, Ottawa, Canada

Abstract

The Si 1s (K-shell) X-ray absorption spectra of a series of strained Si_xGe_{100-x} alloy thin films and several $\{(Si)_m(Ge)_n\}_p$ atomic layer superlattices (ALS) grown epitaxially on Si(100) and Ge(100) substrates have been investigated using plane polarized synchrotron radiation. Polarization dependent components of the signal are attributed to anisotropic states associated with strain-induced tetragonal distortions. The sense of the polarization is shown to be identical for all compositions (x = 25 to 92) of SiGe alloys grown on Si(100) substrates. The opposite polarization dependence is found to occur for all Si_xGe_{100-x} alloys (x = 12 to 50) grown on Ge(100) substrates. The polarization dependence and shape of the near edge spectral features of alloy and ALS samples which have similar (average) chemical composition are remarkably similar. A preliminary comparison of the alloy results with literature band structure calculations is made.

*Address for correspondence:
T. Tyliszczak
Institute for Materials Research,
McMaster University,
Hamilton, Ontario,
Canada L8S 4M1
  Telephone number: (905) 525-9140; extension 24864
  FAX number: (905) 521-2773
  email: tolek@mcmaster.ca

Introduction

Alternating layers of pure Si, pure Ge or variable composition Si_xGe_{100-x} strained single crystal alloys are useful model systems for studying strain in heterostructures and the dependence of materials properties on growth and processing procedures. Such films are currently of interest with regard to quantum engineered electronic structures adapted for specific device applications [7, 9, 17, 20]. Ge K-edge [1, 2, 6, 8, 13, 18, 19, 22, 24, 25] and Si-K edge [10, 11, 12, 24] X-ray absorption spectroscopic measurements have been used to study Si-Ge atomic layer superlattice (ALS) and alloy thin films. The details in the near edge region of X-ray absorption spectra are closely connected to the unoccupied density of states. In particular, Si 1s near edge spectral structure reflects the p-symmetry density of states in the conduction band. Thus, Si 1s absorption spectroscopy provides a probe of an important aspect of the electronic properties of Si-Ge materials. Woicik and Pianetta [24] have outlined the close relationship between X-ray absorption spectra and the structural and electronic properties of Si-Ge systems.

The Si 1s → Si 3p conduction band transitions in crystalline Si_xGe_{100-x} alloys and $\{(Si)_m(Ge)_n\}_p$ ALS samples produce a characteristic double-peaked structure at the Si K-edge [11, 16, 24]. Recently, we have shown that there is a small polarization dependence in the region of this double peaked structure (1838-1844 eV) in the Si 1s near edge spectra of all **strained** alloys and ALS [11, 12]. This polarization dependent signal is absent from the Si 1s spectra of fully **relaxed** alloy and ALS materials, even though the near edge spectra are otherwise quite similar. This polarization dependent signal arises from electronic transitions to anisotropic states which are generated by band splittings caused by the tetragonal distortion. This distortion is the way in which the epitaxial film accommodates the mismatch between the natural (i.e., relaxed) cell sizes of the thin film and the substrate [12]. For commensurate epitaxial growth on Ge(100), the in-plane lattice constant of the growing layer must match that of the Ge substrate. For

the pure Si layers in an ALS or for a Si-rich alloy, this requires an increase in the (Si-Si) in-plane spacing relative to that in a relaxed sample. The interlayer distance then undergoes a corresponding contraction (tetragonal distortion). Thus, in both alloys and ALS grown commensurately on Ge, every Si atom resides in a strained environment in which the in-plane distances are expanded and the out-of-plane distances are contracted relative to pure Si. For commensurate epitaxial growth on Si(100), the sense of the strain is opposite to that experienced by Si atoms deposited on a Ge substrate. That is, the in-plane Ge-Ge distance in the pure Ge layers of an ALS or that in a Ge-rich alloy is contracted, while the out-of-plane distance expands relative to that in pure Ge. The sense of the strain in Si-Ge alloys grown on Si(100) is the same as that in ALS grown on Si(100) but opposite to that in alloys or ALS grown on Ge(100).

Recently, we [11] have shown that a similar polarization effect is seen in the Si 1s spectra of alloys and ALS samples of similar (average) chemical composition grown in a similar way on the same substrate and thus, the anisotropic states are not specific to the abrupt interfaces in the ALS but rather are a property of the extended strain field. In order to more fully explore the polarization dependent effect and its potential use in understanding how the strain in metastable epitaxial structures affects the conduction band structure of Si-Ge electronic materials, we have investigated a series of strained and relaxed alloy films which span a much wider range of compositions than in our earlier study. In addition, a preliminary comparison is made to recent semi-empirical tight-binding calculations of the band structure of strained Si-Ge alloys reported by Ma *et al.* [16].

Experimental

The Si K-edge spectra were recorded using the double crystal beam line [26] at the 1 GeV synchrotron radiation facility of the University of Wisconsin-Madison. The monochromator was equipped with InSb crystals giving a resolution of 0.8 eV at the Si K-edge. After refocussing, the X-ray beam on the sample was approximately 1 mm^2. Total electron yield spectra were obtained using sample current detection. The sampling depth is estimated to be $\approx$ 20 nm, based on a comparison of the relative intensities of oxide to bulk signals in total electron yield and fluorescence yield spectra of a sample of single crystal silicon (c-Si) covered with approximately 2 nm native oxide layer. The incident photon flux (I_o) was monitored using a gas ionization chamber equipped with thin Be windows. Absolute energy scales were established by setting the inflection point of the absorption edge of c-Si (as determined by the peak in the derivative) to 1839.2 eV.
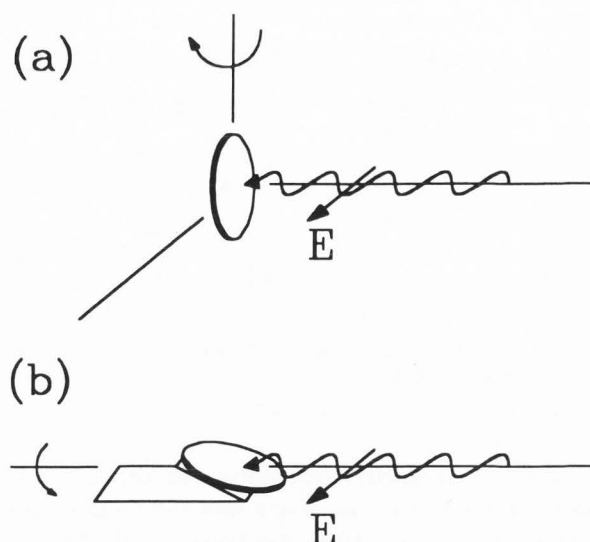

Figure 1. (a) Experimental geometry used for earlier polarization dependent measurements. (b) Geometry used for some of the spectra reported in this work. The relative surface:bulk contribution varies in geometry (a) but is constant in geometry (b).

The polarization dependence (the variation of the spectrum with changes in the angle between the electric vector of the incident radiation and the sample surface) was measured by sample rotation. In earlier measurements [11, 12], the sample rotation was carried out about an axis perpendicular to the X-ray beam (Fig. 1a). In this geometry, the surface of the sample contributes increasingly at grazing incidence. In order to investigate the extent to which the polarization dependent signal could be associated with anisotropic surface states or simply with changing contributions of surface and bulk, a series of measurements were carried out using sample rotation about an axis coincident with the X-ray beam, with the sample surface fixed at 20° relative to the incident beam for all polarizations (Fig. 1b). In this experimental geometry, the relative contributions of the surface and the bulk is the same for all polarizations (based on the estimated 20 nm sampling depth, the surface contribution is $\approx$ 5%). The polarization dependence was found to be very similar for a strained sample measured with both geometries. This suggests the polarization dependent signal is characteristic of the 'bulk' and is not a surface-specific phenomenon. However, in a few cases, surface-related signals were observed which were traced to surface contamination [11]. The absence of polarization dependent signal in fully relaxed samples (see Fig. 4a) is further evidence that any intrinsic surface polarization signal contributes relatively little in the experimental geometries we have used. Finally, in a number of samples, fluorescence yield detection, which
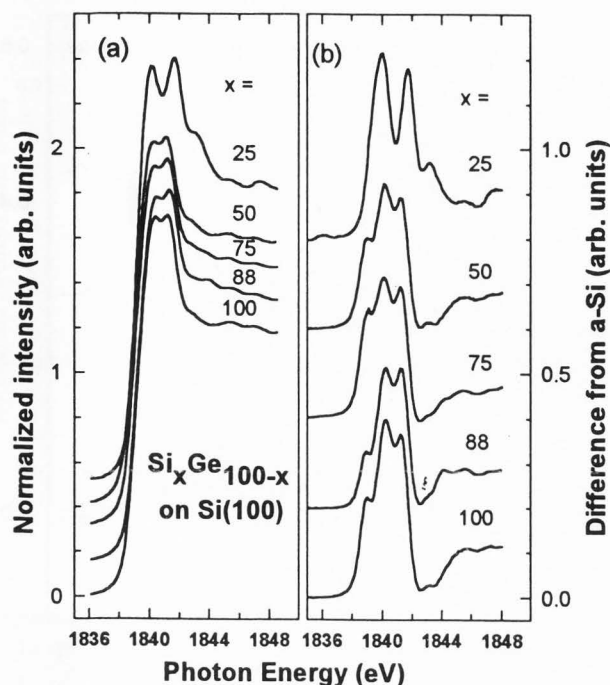
Figure 2. (a) Si 1s spectra of single crystal strained Si-Ge alloys of the indicated composition, grown on Si(100), recorded by total electron yield (sample current) detection. After subtracting a linear background, each spectrum was normalized to unity at 1858 eV. (b) Alloy spectra after subtraction of the spectrum of a-Si, scaled in amplitude and shifted by +0.42 eV. The offsets used to avoid overlap are given by the signal at 1836 eV.

---

samples several micrometers at the Si 1s edge (and therefore, all of the epitaxial film), was found to give identical polarization dependence to that observed with electron yield detection [12].

The single crystal epitaxial layers were grown in a VG Semicon V80 molecular beam epitaxy (MBE) system on Czochralski-grown 100 mm Si(100) or 50 mm Ge(100) wafers with procedures previously described elsewhere [16]. Prior to growth, a thick ($\sim$100 nm) epitaxial Si or Ge buffer layer was grown to ensure identical initial conditions. X-ray diffraction, Raman scattering spectroscopy and cross-section transmission electron microscopy measurements have established the Ge and Si concentrations and nominal layer thicknesses [3, 4, 5]. Most of the alloy samples were > 100 nm thick and thus there was no contribution from the Si(100) substrate. This was not the case for the $Si_{25}Ge_{75}$ and $Si_{50}Ge_{50}$ strained alloys grown on Si(100). For these highly strained species, coherently strained layers can only be grown to a maximum thickness of 10 nm. In these cases, the Si substrate contributes signifi-

cantly to the overall signal. The amorphous Si sample was prepared as described elsewhere [15]. An oxide etch (using 10% HF to remove SiO_x and GeO_x) was carried out just prior to insertion of each sample into the high vacuum chamber where measurements were carried out at a pressure below 2×10^{-7} torr.

Results

Figure 2 compares the Si 1s spectra of a series of Si-Ge alloys with compositions between 25 and 100% Si grown on Si(100). Each spectrum was recorded with the electric vector approximately perpendicular to the surface ($E_\perp$). The spectra have been subjected to a linear background subtraction and normalized to unit intensity at 1858 eV. In addition to the normalized spectra, the part of the near edge signal which is most long-range, and thus most band-structure sensitive, was isolated by subtraction of the spectrum of amorphous Si (a-Si). Prior to subtraction, the a-Si spectrum was shifted by -0.42 eV and unit normalized (see ref. [12] for detailed discussion and rationalization of this alignment procedure). This difference signal is presented in the right hand panel of Figure 2. A clear evolution in spectral shape is evident, with the most obvious developments with increasing Ge content being the increase in the separation of the two peaks at the conduction band maximum (1840-1842 eV) and the growth of a threshold transition at 1839 eV, at least until the Ge content reaches 50%. Woicik and Pianetta [24] have suggested that the compositional dependence of the main peak separation can be understood in terms of a compositional average of the conduction band splitting in pure Si (0.9 eV) and that in a dilute (5% Si) Si-Ge alloy (1.95 eV) which is assumed to approach that of pure Ge. However, this suggestion is not supported by the present results, in that, the splitting does not vary linearly as a function of composition.

Figure 3 plots the Si 1s spectra ($E_\perp$) of alloys grown on Ge(100), with samples covering compositions between 12% and 50% Si. The separation of the two main conduction band peaks is as large or larger than that found in the $Si_{25}Ge_{75}$/Si(100) sample. Again, the evolution of peak separation as a function of composition is not linear, as had been suggested [24]. The threshold feature at 1839 eV is completely absent from the spectra of strained alloys grown on Ge, consistent with an opposite polarization to that in the alloys grown on Si. The small negative intensity at threshold arises because of the choice of alignment of the a-Si and alloy film spectra. A smaller shift of the energy scale of the a-Si spectrum results in a large negative-going signal in the $E_\perp$ spectra of alloys grown on Ge(100) and a reduced size of the 1839 eV threshold peak in that of alloys grown on Si(100).
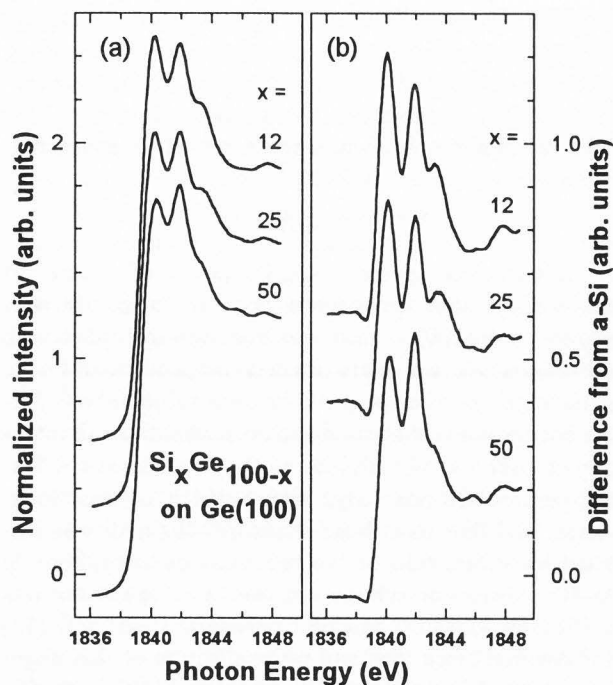
Figure 3. Total electron yield Si 1s spectra of single crystal strained Si-Ge alloys of the indicated composition, grown on Ge(100). **(a)** Background subtracted, normalized spectra recorded with $E_\parallel$. **(b)** Same data after subtraction of the spectrum of a-Si. Data preparation and presentation as for Figure 2.
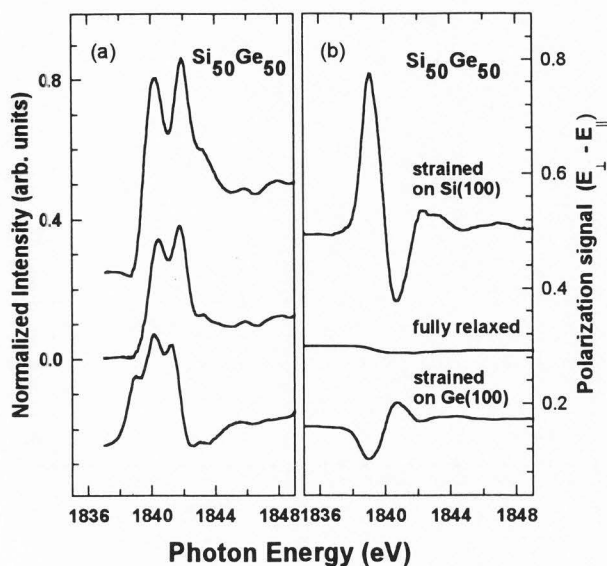

Figure 4 plots the polarization dependent components of the strained alloys grown on Si and Ge. This $(E_\perp - E_\parallel)$ signal is obtained by subtracting the spectrum recorded with the E-vector in the plane of the sample $(E_\parallel)$ from that recorded with the E-vector predominantly along the growth direction $(E_\perp)$. Thus, a positive signal in the difference plot signifies an anisotropic state aligned along the growth direction (z-polarized; out-of-plane; normal to the surface) while a negative signal signifies a state aligned perpendicular to the growth direction {(x,y)-polarized; in-plane; in the plane of the alloy film}. The magnitude of the polarization dependent component indicated by the vertical scale is consistent with the magnitude of the normalized spectra, as indicated in the vertical scales of Figures 2 and 3. Figure 4a also includes the $(E_\perp - E_\parallel)$ difference signal for c-Si in order to demonstrate that the polarization dependence for unstrained samples is much weaker, with the residual likely associated with surface contributions.

If all conduction band states (or their overlap, in the case of unresolved transitions) were isotropic, these $(E_\perp - E_\parallel)$ difference curves should be featureless. Figure 4 shows that, for all compositions of strained alloys grown on Si(100), the lowest energy conduction band
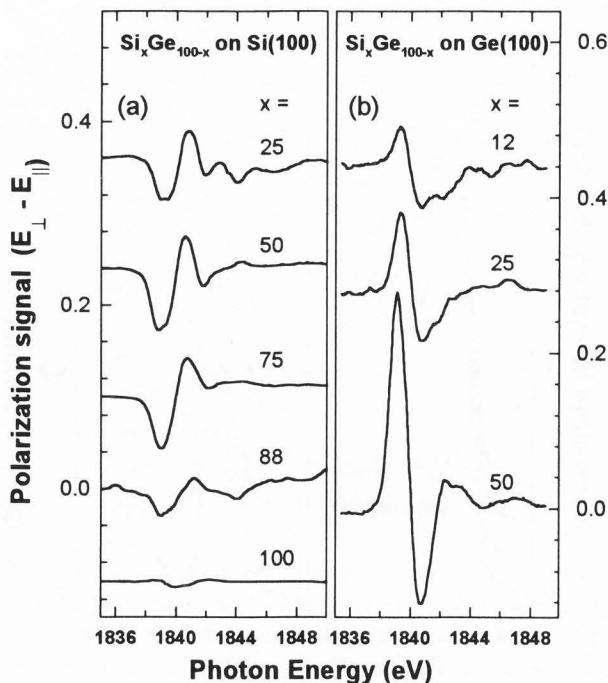
Figure 4. **(a)** Difference between the normalized Si 1s spectra of the strained Si-Ge alloys grown on Si(100) recorded with the E-vector normal from that with the E-vector in the sample plane $(E_\perp - E_\parallel)$. An identical intensity scaling has been used for all plots, with vertical offsets for clarity. The $E_\perp - E_\parallel$ signal for c-Si (recorded in the geometry indicated in Figure 1b is also presented. The small polarization signal for c-Si may be associated with contributions from anisotropic states at the H-terminated surface. **(b)** Polarization dependence $(E_\perp - E_\parallel)$ for strained Si-Ge alloys grown on Ge(100).

---

state (or the net resultant from transitions to a set of overlapping bands) (located at 1839 eV, on the leading edge of the rise in the absorption signal) is (x,y) polarized. In addition, there is a z-polarized signal at 1840.8 eV. Curve fitting suggests this signal arises from a number of z-polarized states [12]). In sharp contrast, the polarization dependent signal in the spectra of the three alloys grown on a Ge(100) substrate is inverted from that of the strained alloys grown on Si(100). In the alloys-on-Ge, the lowest energy state (1839 eV) is strongly z-polarized (and thus did not appear in the $E_\parallel$ spectra plotted in Fig. 3), while there is a more complex (x,y)-polarized signal between 1841 and 1842 eV. In most cases, the polarization component is more intense in strained $Si_xGe_{100-x}/Ge(100)$ than strained $Si_{100-x}Ge_x/Si(100)$ alloy samples (i.e., samples which are of similar compositional mismatch, on opposing substrates). However, we do note that the magnitude of the polarization dependent signal of $Si_{25}Ge_{75}/Ge$ is similar to that of

Figure 5. Comparison of **(a)** amorphous-Si subtracted Si 1s spectra, and **(b)** the polarization dependence ($E_\perp - E_\parallel$), of three $Si_{0.5}Ge_{05}$ alloy samples: **(1)** strained, grown on Ge(100); **(2)** fully relaxed by growth of a very thick film; and **(3)** strained, grown on Si(100).

$Si_{75}Ge_{25}/Si$.

Due to spontaneous relaxation when thicker layers are prepared, the $Si_{25}Ge_{75}/Si(100)$ and $Si_{50}Ge_{50}/Si(100)$ samples could only be grown 10 nm thick. For these species, the polarization dependent intensity is underestimated because there is a significant contribution to the spectrum from the underlying Si(100) substrate. This is the case, despite the fact the polarization dependence is evaluated as a difference, since the $E_\perp$ and $E_\parallel$ spectra are each normalized on a per Si atom basis. Thus

$$I(measured) = \alpha \cdot I(Si_xGe_{100-x}) + (1-\alpha) \cdot I(Si) \tag{1}$$

for both $E_\perp$ and $E_\parallel$, so that

$$(I_\perp - I_\parallel) = \alpha \cdot \{I_\perp(Si_xGe_{100-x}) - I_\parallel(Si_xGe_{100-x})\} \tag{2}$$

and the polarization dependence is reduced by a factor α, the proportion of the total signal coming from the alloy component of the $Si_xGe_{100-x}/Si(100)$ epitaxial film. Assuming $\alpha = 0.5$ (i.e., a 10 nm thick epitaxial film measured using a total electron yield sampling depth of 20 nm), the real polarization dependence for the $Si_{25}Ge_{75}/Si(100)$ and $Si_{50}Ge_{50}/Si(100)$ samples should be twice as large as that given in Figure 4, which would make them much more comparable in magnitude to that for the corresponding alloy films grown on Ge. We plan to measure these samples using a partial yield detection mode under ultra high vacuum (UHV) condi-

tions. This should result in a depth sensitivity less than the thickness of the strained alloy layer. Measurements under UHV conditions will also enable us to explore the Si 1s spectrum of the surface.

The results shown in Figure 4 are fully consistent with our earlier studies of Si 1s spectra of strained alloys [11]. They clearly show that the polarization dependence is dictated by the nature of the substrate (and thus, the orientation of the strain field in the epitaxial film). Although the magnitude and detailed shape of the polarization signal varies somewhat, the sense of the polarization dependent signal is **independent** of alloy composition.

Figure 5 compares the long-range components of the near edge spectra (isolated by subtraction of the a-Si signal) and the polarization dependence of three different 50:50 alloy samples: strained $Si_{50}Ge_{50}$ grown on Si(100), strained $Si_{50}Ge_{50}$ grown on Ge(100), and a $Si_{50}Ge_{50}$ film grown to several micrometers thickness on Si(100) which is not strained (i.e., completely relaxed). This comparison dramatically illustrates the dominant role of the substrate in determining the conduction band structure of the alloy film. Not only is the polarization dependence inverted (right hand panel), but there are also changes in the overall spectral shape (left hand panel). While some of the spectral shape changes are simply a consequence of comparing $E_\perp$ spectra of oppositely polarized samples, other changes (e.g., those around 1843 eV) can only be explained as changes in the isotropic components of the band structure both as a function of the nature of the substrate and as a function of the presence or absence of strain. Crudely speaking, one might have expected the isotropic component to be rather similar in these three samples. However, this assumes a similar sensitivity of the band structure to tensile versus compressive stress. The variation in the isotropic component, which can be obtained by making measurements at the angle where the spectrum is independent of polarization (E-vector at 54.3° relative to the surface [21]), would be a more accurate measure of the differences in the sensitivity of the conduction band to tensile versus compressive stress.

Some of the difference in amplitudes of the polarization dependent signals of strained alloys grown on Ge versus those grown on Si is a result of the difference in elastic stiffness constants for Ge and Si. For the case of dilute alloys, the difference in the orthogonal components of the strain tensor ($\epsilon_\perp - \epsilon_\parallel$) for Ge in Si on Ge is 30% larger than for Si in Ge on Si because of differences in the elastic stiffness constants [16]. While the relationship between magnitude of polarization dependence and strain anisotropy is not yet quantified, this effect is consistent with a larger polarization dependence for alloys grown on Ge than those grown on Si. Since

the $(\epsilon_\perp - \epsilon_\parallel)$ values for on-Si and on-Ge alloys will differ by a smaller amount for more concentrated alloys, the polarization dependent signal of corresponding on-Si and on-Ge alloys should become more similar as the composition approaches 50:50.

As illustrated in Figure 6, the shape of the near edge spectra as well the polarization dependent component of the Si 1s signal from Si-Ge atomic layer superlattices is essentially the same as that for an alloy of a composition equal to the average composition of the ALS. A rationale for this equivalence has been previously given [11]. While some of this similarity can be attributed to interface mixing, and thus, some alloy-like character to the ALS samples, the similarity of the ALS and alloy Si 1s spectra reflects the sensitivity of these near edge signals to the **long range** aspects of the electronic structure. The long range aspect is dictated by the strain field (which seems to be a property of the whole strained film and is similar in similar-composition ALS and alloys), rather than the immediate first shell environment of the core-excited Si atom (which differs significantly between alloy and ALS samples).

Discussion

A striking feature of these results (e.g., Figs. 5 and 6) is the reversal of polarity of the polarization dependent signal between alloy and ALS samples grown on Si and those grown on Ge. This confirms that the polarization effect in both the alloy and the ALS samples is directly related to long range strain. The desirable properties of the strained Si-Ge materials for electronic applications arise from the influence of strain on the band structure. In principle, our results can provide useful experimental tests for the accuracy of various schemes to calculate the band structure and other electronic properties of strained alloys and superlattices. These experimental results can be related to theory by using the partial density of states of p-symmetry as a first order estimate of the Si 1s spectral structure. This approach ignores the influence of the core hole and possible variations of the transition matrix element in the threshold region. Both of these factors are believed to be relatively small effects for the 1s spectra of covalently bonded group IV elements [23]. Unfortunately, we have not been able to find partial density of states calculations for strained Si_xGe_{100-x} alloys or superlattices in the literature.

As a first attempt to connect our results to theory, we have used the alloy band structure information provided by the tight binding calculations of Ma et al. [16]. Note that the alloys are denoted as $Si_{1-x}Ge_x$ in ref. [16], so that, their compositional variable, x, refers to the Ge content rather than the Si content, as we have used in
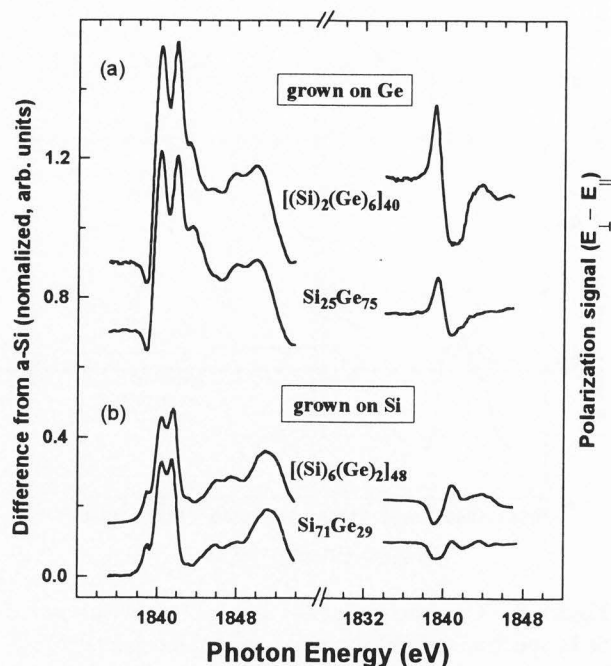
Figure 6. Comparison of the shape (amorphous-Si subtracted, left side) and polarization dependence $\{(E_\perp - E_\parallel)$, right side\} of the Si 1s spectra of strained alloys and strained $\{(Si)_m(Ge)_n\}_p$ atomic layer superlattices of similar composition, grown on (a) Ge(100) and (b) Si(100). The vertical scales are the same for both parts of the figure. The offsets used to avoid overlap are given by the signal at 1836 eV.

----

this work. According to the results of Ma et al. [16], the lowest energy conduction band state for alloys grown on Si(100) is the in-plane, (x,y)-polarized $E_c^\Delta(4)$ band (see Fig. 6 of ref. [16]). The out-of-plane, z-polarized $E_c^\Delta(2)$ band occurs at a few tenths of an eV higher energy, with the $E_c^\Delta(4)-E_c^\Delta(2)$ separation increasing as the Ge content of the alloy increases. At slightly higher energy (0.2-0.8 eV), there is the in-plane, $E_c^L(4)$ band. Since our experimental resolution is only 0.8 eV and the 1839 eV polarization dependent signal has a width of 1.4 eV (FWHM), it is most likely the three lowest bands predicted by the Ma et al. [16] calculation would all overlap in the "1839 eV" band. Indeed, there are signs of a 0.4-0.6 eV splitting at the top of the "1839 eV" signal in the x = 25, 50 and 88 alloy samples (Fig. 4a) which could correspond to the separation of the $E_c^\Delta(4)$ and $E_c^L(4)$ bands. Thus, even though the p character of the bands or the matrix elements have not been considered, this simple comparison with the band edge positions does suggest the signal at the threshold of the Si 1s → conduction band transitions should be dominated by (x,y), in-plane polarized states, consistent with our results.

The Ma *et al.* [16] calculations indicate that the lowest energy conduction band state for alloys grown on Ge(100) is the out-of-plane, z-polarized $E_c^\Delta(2)$ band for alloys with a Ge content of less than 50% (see Fig. 7 of ref. [16]). However, for alloys richer in Ge (i.e., for all of the samples studied in this work), the lowest energy band is predicted to be the in-plane, (x,y)-polarized $E_c^L(4)$ band. The in-plane polarized $E_c^\Delta(4)$ band occurs at slightly higher energy (<0.5 eV). Thus, Ma *et al.* [16] predict that the dominant character of the first 0.5 eV of the conduction band of alloys grown on Ge(100) is **in-plane** polarized. Since our experimental results indicate unequivocally that there is a strong **out-of-plane**, z-polarization to the first 1 eV of the conduction band (see Fig. 4b), there appears to be a fundamental disagreement between experiment and theory for strained Si-Ge alloys grown on Ge(100).

One possible explanation of this discrepancy could be that in the alloys grown on Ge(100), the matrix element for the Si 1s $\rightarrow E_c^\Delta(2)$ transition could be much larger than that for the Si 1s $\rightarrow E_c^\Delta(4)$ and Si 1s $\rightarrow E_c^L(4)$ transitions. However, if this was the case, the matrix elements for transitions in alloys grown on Si(100) would be expected to be similar, resulting in a z-polarized lowest energy signal in the alloys grown on Si. Knowledge of the Si 3p character of these individual bands would allow some estimates of the relative matrix elements, since to zeroth order, the matrix element is proportional to the Si 3p content of the conduction band. Another difficulty with this simple comparison is that Ma *et al.* [16] indicate only the band edge and not the density of states for each band, integrated over all values of the momentum of the electron in that band. If this more detailed information was available for the first 10 eV above the conduction band edge, a meaningful comparison with our results could be made.

Summary

The Si 1s spectra of a series of Si_xGe_{100-x} alloy films grown epitaxially on Si(100) and Ge(100) have been recorded at high resolution and with variable polarization. The spectral shape and polarization signal are most strongly related to the nature of the substrate and thus the spatial orientation of the strain. Both the spectral shape and the polarization dependence for ALS and alloys of similar average composition are very similar. A preliminary comparison to band structure calculations of strained epitaxial alloys [16] has been made. However, as yet, insufficient information is available about these calculations to make a meaningful comparison to our results. This will require knowledge of the p symmetry density of states over the region of the polarization dependent threshold signal. Ideally, this should also include a consideration of the matrix elements and possible influence of the core hole on the excited state electronic structure [14]. With this information, it should be possible to quantitatively relate these Si 1s experimental measurements to the fundamental electronic properties of these strained Si-Ge materials.

Acknowledgements

References

1. Aebi P, Tyliszczak T, Hitchcock AP, Jackman TE, Baribeau JM (1991) X-ray absorption fine structure studies of buried Ge-Si interfaces. J. Vac. Sci. Tech. A **9**: 907-911.

2. Aebi P, Tyliszczak T, Hitchcock AP, Baines KM, Sham TK, Jackman TE, Baribeau JM, Lockwood DJ (1992) Simultaneous analysis of multiple extended X-ray absorption fine structure spectra: Application to studies of buried Ge-Si interfaces. Phys. Rev. B **45**: 13579-13590.

3. Baribeau JM (1988) X-ray double crystal characterization of molecular beam epitaxially grown $Si/Si_{1-x}Ge_x$ strained-layer superlattices. Appl. Phys. Lett. **52**: 105-107.

4. Baribeau JM (1990) Low angle x-ray reflection study of ultrathin Ge films on (100)Si. Appl. Phys. Lett. **57**: 1748-1750.

5. Baribeau JM, Lockwood DJ, Dharna-wardana MWC, Rowell NL, McCaffrey JP (1989) Growth and characterization of SiGe atomic layer superlattices. Thin Sol. Films **183**: 17-24.

6. Baribeau JM, Lockwood DJ, Jackman TE, Aebi P, Tyliszczak T, Hitchcock AP (1991) Characterization of ultra-thin Ge epilayers on (100) Si. Can. J. Phys. **69**: 246-254.

7. Bean JC, Kasper E (1988) Silicon Molecular Beam Epitaxy. CRC Press, Boca Raton, FL. pp. 11-47.

8. Bouldin CE (1989) EXAFS study of buried Ge layers in silicon. Physica B **158**: 596-597.

9. Fasol G, Fasolino A, Lugli P (1989) Spectroscopy of Semiconductor Microstructure. Plenum, NY. pp. 65-73.

10. Hitchcock AP, Tyliszczak T, Aebi P, Sham TK, Baines KM, Xiong JZ, Mueller KA, Feng XH, Chen JM, Yang BX, Lu ZH, Baribeau JM, Jackman TE (1993) Si K-edge and Ge K-edge X-ray absorption spectroscopy of the Si-Ge interface in $[(Si)_m(Ge)_n]_p$ atomic layer superlattices. Surf. Sci. **291**: 349-369.

11. Hitchcock AP, Tyliszczak T, Rocco MLM, Francis JT, Urquhart SG, Feng XH, Lu ZH, Baribeau JM, Jackman TE (1994) Polarization dependence of the Si 1s X-ray absorption spectra of single crystal Si-Ge alloys and atomic layer superlattices. J. Vac. Sci. Tech. A **12**: 1142-1147.

12. Hitchcock AP, Tyliszczak T, Aebi P, Feng XH, Lu ZH, Baribeau JM, Jackman TE (1994) Polarization dependence of the Si 1s X-ray absorption spectra of Si-Ge atomic layer superlattices. Surf. Sci. **301**: 260-272.

13. Jackman TE, Baribeau JM, Lockwood DJ, Aebi P, Tyliszczak T, Hitchcock AP (1992) Thermal stability of the $(Si_mGe_n)_p$ superlattice interface. Phys. Rev. B. **45**: 13591-13594.

14. Jollet F, Noguera C (1993) Core hole effect on the XAS Si K edge shape in α-quartz. phys. stat. sol. B **179**: 473-488.

15. Lu ZH, Poulin-Dandurand S, Sacher E, Yellin A (1990) Ge configurations in hydrated amorphous silicon as studied by X-ray photoemission spectroscopy. Phys. Rev. B **42**: 5186-5190.

16. Ma QM, Wang KL, Schulman JN (1993) Band structure and symmetry analysis of coherently grown $Si_{1-x}Ge_x$ alloys on oriented substrates. Phys. Rev. B **47**: 1936-1953.

17. Meyerson BE (1994) Ultrahigh-vacuum CVD process makes SiGe devices. Sol. State Technol. **37**(2); 53-55.

18. Oyanagi H (1992) Monolayer superlattices and heterostructures studied by surface-sensitive XAFS. Appl. Surf. Sci. **60/61**: 522-528.

19. Oyanagi H, Sakamoto T, Sakamoto K, Matsushita T, Yao T, Isheguro T (1988) Si/Ge/Si monolayer heterostructures on Si(100) studied by surface-sensitive EXAFS. **57**: 2086-2092.

20. Pearsall TP (1991) Si-Ge alloys and superlattices for optoelectronics. Mat. Sci. Eng. B **9**: 225-231.

21. Stöhr J (1993) NEXAFS Spectroscopy, Springer Tracts in Surface Science **25**: Springer, Berlin. p. 284.

22. Tyliszczak T, Aebi P, Hitchcock AP, Jackman TE, Baribeau JM, Lockwood DJ (1993) Simultaneous multiple file EXAFS analysis: Methodology and application to buried Ge-Si interfaces. Jap. J. Appl. Phys. **32**: 134-136.

23. Weng X, Rez P, Sankey OF (1989) Pseudo-atomic orbital band theory applied to electron energy loss near-edge structures. Phys. Rev. B **40**: 5694-5704.

24. Woicik JC, Pianetta P (1992) Studies of Si-Ge interfaces with surface EXAFS and photoemission. In: Synchrotron Radiation Research: Advances in surface and Interface Science, Vol. 2. Issues and Technology. Bachrach RZ (ed.). Plenum, NY. pp. 211-266.

25. Woicik JC, Bouldin CE, Bell MI, Cross JO, Tweet DJ, Swanson BD, Zhang TM, Sorensen LB, King CA, Hoyt JL, Pianetta P, Gibbons JF (1991) Conservation of bond lengths in strained Ge-Si layers. **43**: 2419-2422.

26. Yang B.X, Middleton F, Olssen B, Bancroft G.M, Chen JM, Sham TK, Tan KH, Wallace D (1992) Double crystal monochromator beam line on the Aladdin 1-GeV storage ring. Rev. Sci. Inst. **63**: 1355-1358.

Discussion with reviewers

D. McComb: The authors should present at least one example of a spectrum collected with $\epsilon_\|$ to convince the reader of the quality of the data acquired. It would also be worthwhile to show that the difference spectrum for Si_xGe_{100-x} on Si(100) or Ge(100) is indeed featureless when x = 100 or x = 0, respectively.

Authors: Detailed presentations of $\epsilon_\perp$ and $\epsilon_\|$ data have been given in two recent articles [11, 12] from our group. The quality of the difference curves clearly indicates that the $\epsilon_\|$ spectra are of similar statistical quality. The difference spectrum for c-Si {equivalent to unstrained Si_xGe_{100-x} on Si(100), x = 100} in Figure 4a demonstrates the absence of polarization dependence signal. There is no Si to detect in x = 0 samples and samples of Si_xGe_{100-x} x = 100 on Ge(100) were not available. Therefore, neither of these two cases can be dealt with.

D. McComb: The splitting of the "1839 eV" signal is absent in the x = 75 sample but is present in all of the other compositions (see Fig. 4a). Please comment on this discrepancy.

Authors: While it is true that a splitting is not observed for x = 75 in Figure 4a, simultaneous curve fitting of the sequence of four alloy spectra plotted in Figure 4a does support the existence of two components separated by an energy spacing similar to that in the x = 25 and x = 50 samples.